

SHORT COMMUNICATION

Peptidomimetic ethyl propenoate covalent inhibitors of the enterovirus 71 3C protease: a P2–P4 study

Melgious J. Y. Ang¹, Qiu Ying Lau¹, Fui Mee Ng¹, Siew Wen Then¹, Anders Poulsen¹, Yuen Kuen Cheong¹, Zi Xian Ngho¹, Yong Wah Tan², Jianhe Peng¹, Thomas H. Keller¹, Jeffrey Hill¹, Justin J. H. Chu^{2,3}, and C. S. Brian Chia¹

¹Experimental Therapeutics Centre, Agency for Science, Technology and Research (A*STAR), Singapore, ²Institute of Molecular and Cell Biology, Agency for Science, Technology and Research (A*STAR), Singapore, and ³Laboratory of Molecular RNA Virology and Antiviral Strategies, Department of Microbiology, National University of Singapore, Singapore

Abstract

Enterovirus 71 (EV71) is a highly infectious pathogen primarily responsible for Hand, Foot, and Mouth Disease, particularly among children. Currently, no approved antiviral drug has been developed against this disease. The EV71 3C protease is deemed an attractive drug target due to its crucial role in viral polyprotein processing. Rupintrivir, a peptide-based inhibitor originally developed to target the human rhinovirus 3C protease, was found to inhibit the EV71 3C protease. In this communication, we report the inhibitory activities of 30 Rupintrivir analogs against the EV71 3C protease. The most potent inhibitor, containing a P2 ring-constrained phenylalanine analog (compound **9**), was found to be two-fold more potent than Rupintrivir (IC₅₀ value 3.4 ± 0.4 versus 7.3 ± 0.8 μM). Our findings suggest that employing geometrically constrained residues in peptide-based protease inhibitors can potentially enhance their inhibitory activities.

Keywords

3C protease, EV71, peptide-based inhibitor, Rupintrivir

History

Received 3 January 2015
Revised 31 January 2015
Accepted 2 February 2015
Published online 20 March 2015

Introduction

Enterovirus 71 (EV71) is a single-stranded, positive-sense RNA virus belonging to the genus *Enterovirus*, family *Picornaviridae*¹. This highly infectious pathogen is spread through the oral-fecal route and is primarily responsible for Hand, Foot, and Mouth Disease (HFMD) in humans, particularly young children, with outbreaks occurring in the Asia-Pacific region including Australia, China, Malaysia, Singapore, Taiwan, Thailand and Vietnam². Infection symptoms include fever, vomiting, vesicular rashes on the hands, feet, buttocks, and oropharyngeal ulcers³. Although the disease is generally self-limiting, a small percentage of patients develop severe neurological complications including encephalitis, aseptic meningitis, and poliomyelitis-like flaccid paralysis^{2,4}. The virus is highly contagious; a 2008 outbreak in China resulted in 488 955 human infections with 126 fatalities⁵ and, more recently, a 2011 outbreak resulted in more than 1.6 million human infections causing more than five hundred deaths⁶. These grim statistics highlight an urgent need for the development of antivirals against EV71 as there is a current lack of effective drugs for treating this disease^{2,6}.

An appealing drug target is the viral 3C cysteine protease which plays a crucial role in cleaving virus-encoded polyproteins

into mature viral proteins specifically at the polyprotein's Gln–Gly peptide bond junction^{6,7}. Indeed, peptidomimetics mimicking the protease's recognition substrate ALFQ-X, with 'X' representing a reactive electrophile like an aldehyde or an acrylate Michael acceptor, have been shown to inhibit the EV71 3C protease^{8–10}. Rupintrivir (AG-7088; Figure 1A), a peptide-based drug candidate with an electrophilic ethyl propenoate Michael acceptor at its C-terminus, was originally developed as a human rhinovirus virus (HRV) 3C protease inhibitor by Agouron Pharmaceuticals^{12–15}. Recently, Rupintrivir showed promising results when used for treating EV71-infected mice¹⁶. The rationale for this was because HRV, like EV71, belongs to the same *Picornaviridae* family of viruses, suggesting that a viral protease inhibitor developed for HRV might also be effective on EV71¹². When bound to the viral 3C protease active site, the ethyl propenoate moiety reacts with the protease's nucleophilic Cys147–SH via a Michael addition to form an S–C covalent bond, irreversibly inhibiting the protease. Indeed, this mechanism of action was further supported by X-ray crystallography studies using co-crystals of Rupintrivir bound to the EV71 3C protease^{9,10}. However, it must be emphasized that Rupintrivir was originally optimized to target the HRV 3C protease and not EV71. A primary sequence comparison between the two viral proteases revealed a 43% sequence identity over 183 residues, suggesting that there might be room for further structural optimization for the EV71 3C protease. In this structure–activity relationship (SAR) study, we report the synthesis and inhibitory activities (IC₅₀) of 30 Rupintrivir analogs against the EV71 3C protease.

Address for correspondence: C. S. Brian Chia, Experimental Therapeutics Centre, Agency for Science, Technology and Research (A*STAR), 31 Biopolis Way, Nanos #03-01, Singapore 138669, Singapore. Tel: +65 64070348. Fax: +65 64788768. E-mail: cschia@etc.a-star.edu.sg

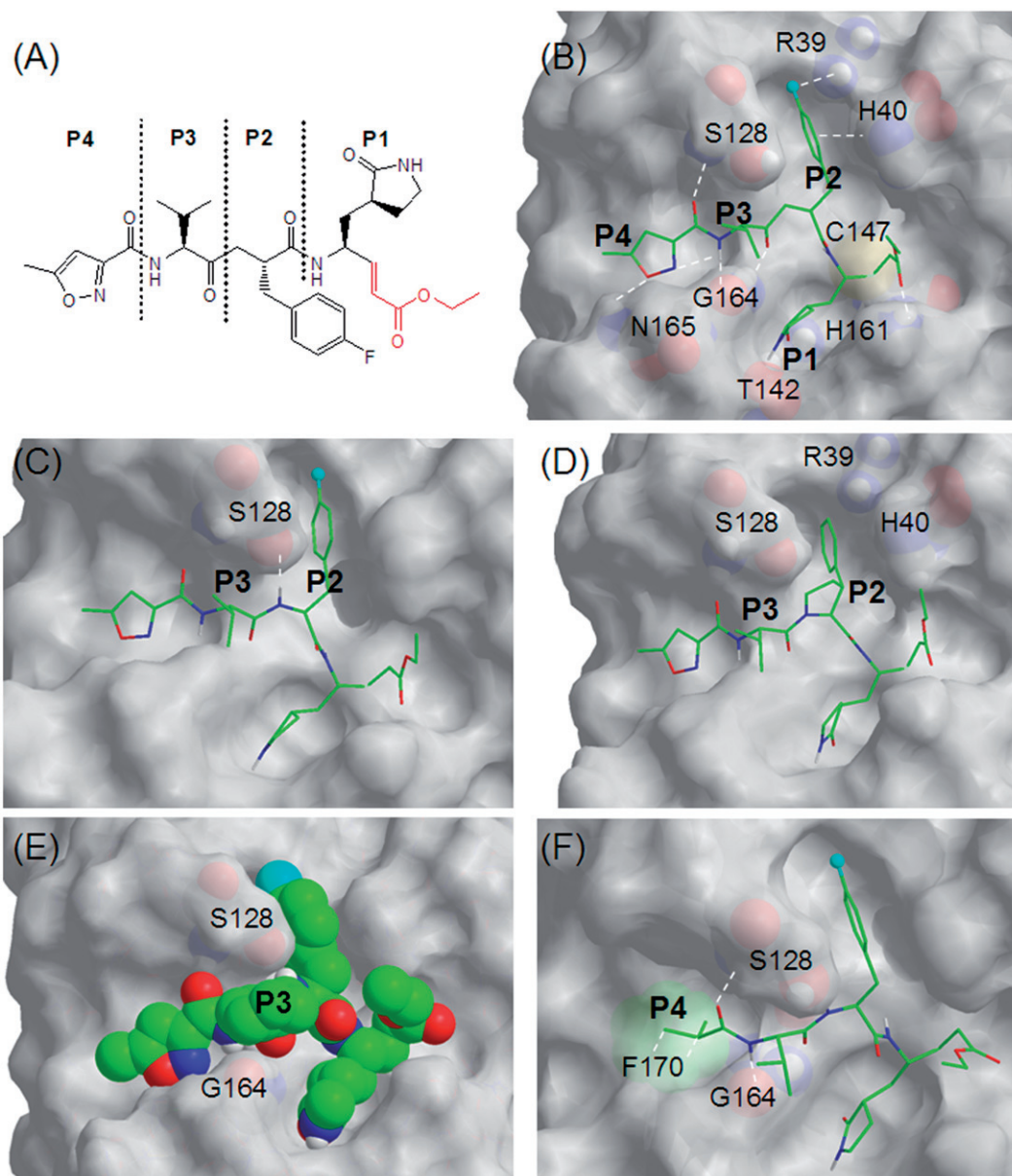


Figure 1. (A) Schematic diagram of Rupintrivir showing P1, P2, P3, and P4 regions using conventional terminology¹¹. The ethyl propenoate moiety is depicted in red; (B) the stick model of Rupintrivir (green) in the EV71 3C protease catalytic site (3SJO.pdb). Protease residues involved in ligand interaction are numbered and shown as CPK representations, the cyan sphere represents fluorine and white hashes represent possible interactions; (C) Cpd. 2 showing the extra H-bond between the P2 NH and S128; (D) Cpd. 9 with its P2 phenylpyrrolidine moiety oriented in the S2 subsite; (E) the CPK model of Cpd. 16 showing its P3 cyclohexyl sandwiched between S128 and G164; (F) Cpd. 21 showing hydrophobic interactions between its P4 N-cap and F170 phenyl group (green CPK representation) in the S4 subsite. Figures C–F were obtained from molecular modeling.

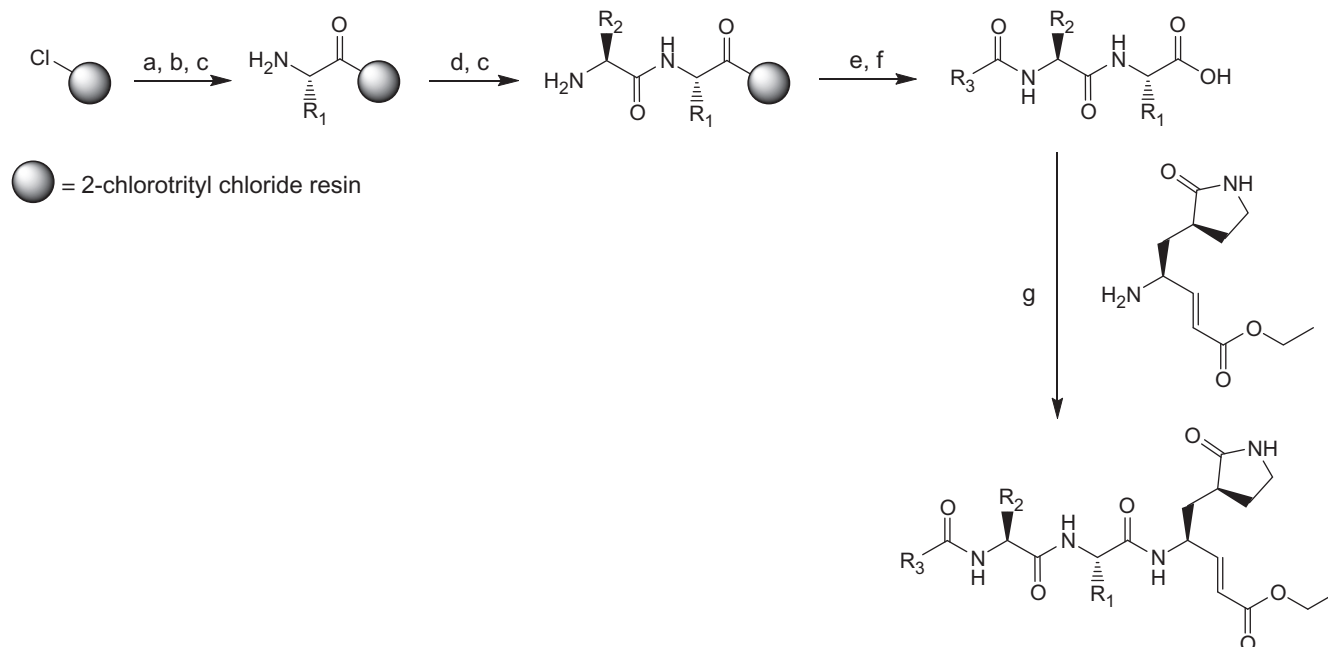
Methods

The general synthetic procedure for compounds **2–31** is outlined in Scheme 1. Detailed synthetic protocols and spectral data can be found in the Supplementary notes. Inhibitory activities of the synthesized peptidomimetics were generated using a published EV71 3C protease inhibition assay¹⁷ (see Supplementary information for details) and are summarized in Table 1. Molecular modeling and energy minimization were performed using Macromodel 9.9 (Schrödinger, New York, NY) (see Supplementary information for details).

Results and discussion

Rupintrivir (compound **1**; Figure 1A), used as a reference in this study, possessed an IC_{50} value of $7.3 \pm 0.8 \mu M$ against the EV71 3C protease (Table 1), close to the $2.3 \pm 0.5 \mu M$ previously reported¹⁰. A structure of Rupintrivir bound to the

EV71 3C protease active site obtained using X-ray crystallography (Figure 1B; 3SJO.pdb)⁹ revealed several noteworthy features: (a) the overall protease active site was relatively shallow with the exception of the S1 and S2 subsites; (b) the catalytic Cys147 formed a S–C covalent bond to the inhibitor's ethyl propenoate moiety; (c) the S1 subsite appeared to accommodate a 5-membered lactam well with H-bonding interactions to Thr142 and His161 of the protease; (d) the relatively narrow S2 subsite could accommodate the P2 phenyl and is involved in π – π interactions with His40 while the aromatic *para*-F was likely involved in electrostatic interactions with the cationic Arg39; (e) the S3 subsite was located above the inhibitor backbone, sandwiched between protease residues Ser128 and Gly164 with the P3 sidechain being solvent-exposed; (f) the S4 subsite spanned a relatively large but shallow area, suggesting that the potential for further P4 optimization might be somewhat limited.



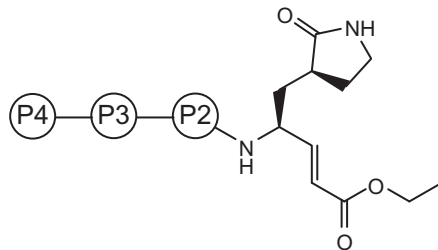
Scheme 1. General synthetic procedure for compounds **2–31**. Reagents and conditions: (a) swell 2-chlorotrityl chloride resin in DMF, 25 °C, 30 min; (b) appropriate Fmoc-protected amino acid: Fmoc-R₁-OH, DIPEA, CH₂Cl₂, 25 °C, 30 min; (c) 20% piperidine in DMF (v/v), 25 °C, 30 min; (d) appropriate Fmoc-protected amino acid: Fmoc-R₂-OH, HBTU, HOBT, DIPEA, DMF, 25 °C, 1 h; (e) appropriate carboxylic acid: R₃COOH, HBTU, HOBT, DIPEA, DMF, 25 °C, 1 h; (f) 95% TFA in CH₂Cl₂ (v/v), 25 °C, 30 min; (g) (*S,E*)-ethyl 4-amino-5-(*S*-2-oxopyrrolidin-3-yl)pent-2-enoate, DIC, HOBT, DMF, 25 °C, 16 h.

Our SAR study started with the P2 residue. The first analog, compound **2** (Table 1), was identical to Rupintrivir except that the backbone methylene between P2 and P3 was substituted with NH (Figure 1C). Surprisingly, this did not significantly affect its IC₅₀ value compared with Rupintrivir (IC₅₀ value 6.2 ± 0.6 versus 7.3 ± 0.8 μM), suggesting that the additional hydrogen bond between the P2 and P3 amide NH to the Ser128 side-chain hydroxyl did not play a significant role in binding (Figure 1C). We next moved the aromatic *para*-F to the *ortho*- and *meta*-positions (compounds **3** and **4**, respectively) and observed approximate two-fold reduction in inhibitory activities (Table 1). This suggested that the protease preferred a *para*-F and that the electrostatic-like interaction between the *para*-F to Arg39 played an important role in inhibitor binding. We further tested this hypothesis by removing the fluorine (compound **5**). As expected, a two-fold reduction in inhibitory activity was observed compared with compound **2** (IC₅₀ value 13.0 ± 1.9 versus 6.2 ± 0.6 μM, respectively; Table 1). Substituting the *para*-F with *para*-trifluoromethyl and *para*-carboxyl moieties (compounds **6** and **7**, respectively) yielded interesting results; the *para*-CF₃ (compound **6**) substitution resulted in similar activity to *para*-F (compound **2**) with IC₅₀ values of approximately 6 μM while the *para*-COOH (compound **7**) substitution abrogated inhibitory activity (IC₅₀ value >100 μM), suggesting that the carboxyl group was too large to fit into the S2 subsite. To further explore the S2 subsite specificity, we replaced the P2 phenyl with a 5-membered thiophene (compound **8**), a known phenyl group bioisostere¹⁸. Intriguingly, this improved inhibition almost two-fold compared to the P2 phenylalanine of compound **5** (IC₅₀ value 7.5 ± 0.9 versus 13.0 ± 1.9 μM), suggesting that thiophene was a suitable bioisostere for phenylalanine. In our final P2 analog, we substituted the P2 phenylalanine with a 3-phenylpyrrolidine moiety which could be considered as a geometrically constrained phenylalanine analog (compound **9**; Table 1). Interestingly, assay results revealed it to be approximately four-fold more potent than

compound **5** with a P2 phenylalanine (IC₅₀ value 3.4 ± 0.4 versus 13.0 ± 1.9 μM) and two-fold more potent than the reference compound Rupintrivir (IC₅₀ value 3.4 ± 0.4 versus 7.3 ± 0.8 μM). Molecular modeling^{19–21} suggested that the 5-membered pyrrolidine moiety could fit into the active site with the phenyl ring optimally oriented in the S2 subsite (Figure 1D). In addition, the highly constrained ring structure could have played a significant role in reducing the entropic binding penalty, resulting in a two-fold increase in inhibitory activity over Rupintrivir. This finding could potentially open avenues towards the design of new peptidomimetic inhibitors containing geometrically constrained phenylalanine surrogates.

We next shifted our focus to the P3 residue. Close inspection of the X-ray crystal (3SJO.pdb) of Rupintrivir's P3 valine residue revealed that its N-terminal NH and C-terminal CO were involved in H-bonding to Gly164 while the *iso*-propyl side-chain was flanked by Ser128 and Gly 164 and was mainly solvent exposed (Figure 1B). Thus, any P3 variation was not expected to affect IC₅₀ values significantly. Surprisingly, our analog with a P3 glycine (compound **10**; Table 1) caused a five-fold decrease in inhibitory activity compared with compound **2** (32.8 ± 4.1 versus 6.2 ± 0.6 μM). We postulated this to be due to the higher entropy penalty paid on ligand-protease binding since glycine, lacking a side-chain, was significantly more flexible than valine in compound **2** (Table 1). Replacing the P3 valine with alanine (compound **11**) altered the IC₅₀ value slightly (7.7 ± 0.5 versus 6.2 ± 0.6 μM), while an amino *iso*-butyric acid residue replacement (compound **12**) resulted in a two-fold decrease in inhibitory activity over compound **2** (13.4 ± 1.1 versus 6.2 ± 0.6 μM). The latter result suggested that the P3 subsite was too small to fit an extra α-methyl group. Replacing the P3 valine with more bulky residues (compounds **13–19**; Table 1) proved detrimental to inhibitory activities (Table 1). For example, substituting the P3 valine with cyclohexylglycine (compound **16**) resulted in a three-fold decrease in inhibitory activity over compound **2** (18.3 ± 1.7

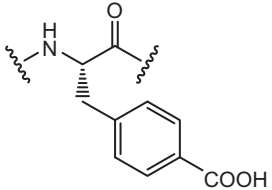
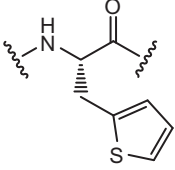
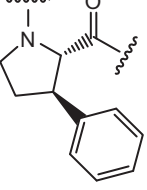
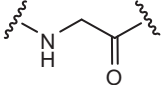
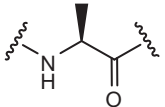
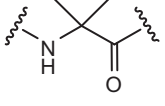
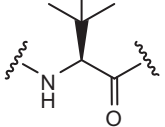
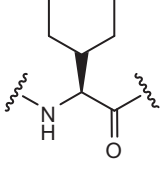
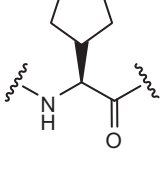
Table 1. Structures and inhibitory data of Rupintrivir analogs against EV71 3C protease.



#	P4	P3	P2	IC ₅₀ (μM)
1				7.3 ± 0.8
2				6.2 ± 0.6
3				14.9 ± 2.1
4				12.9 ± 1.5
5				13.0 ± 1.9
6				6.0 ± 0.8

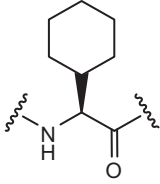
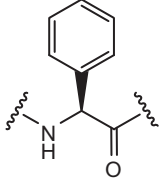
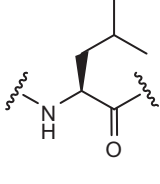
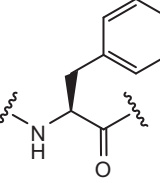
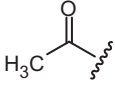
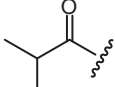
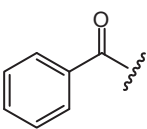
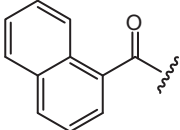
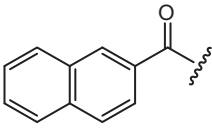
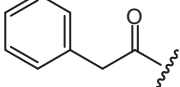
(continued)

Table 1. Continued

#	P4	P3	P2	IC ₅₀ (μM)
7				>100
8				7.5 ± 0.9
9				3.4 ± 0.4
10				32.8 ± 4.1
11				7.7 ± 0.5
12				13.4 ± 1.1
13				9.3 ± 0.8
14				12.7 ± 1.2
15				13.7 ± 1.1
16				18.3 ± 1.7

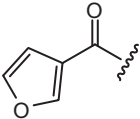
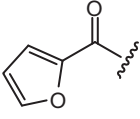
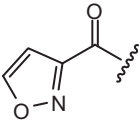
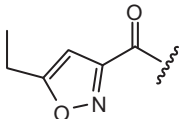
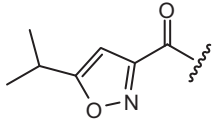
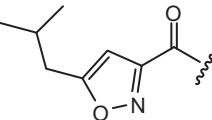
(continued)

Table 1. Continued

#	P4	P3	P2	IC ₅₀ (μM)
				
17				14.2 ± 1.3
18				10.5 ± 1.0
19				12.2 ± 0.9
20				9.5 ± 0.7
21				7.2 ± 0.6
22				15.7 ± 1.9
23				16.8 ± 2.7
24				33.3 ± 3.7
25				12.9 ± 1.4
26				9.3 ± 0.7

(continued)

Table 1. Continued

#	P4	P3	P2	IC ₅₀ (μM)
				
27				16.1 ± 1.9
28				7.0 ± 0.9
29				8.5 ± 0.9
30				8.7 ± 1.5
31				8.3 ± 1.6

versus $6.2 \pm 0.6 \mu\text{M}$; Table 1). Molecular modeling suggested it to be due to unfavorable steric hindrance between the cyclohexyl ring and flanking residues Ser128 and Gly164 (Figure 1E).

Our final series of analogs involved varying the P4 N-cap. In Rupintrivir, this was represented by a 5-methylisoxazole-3-carbonyl moiety (compound **1**; Table 1). Closer inspection of Figure 1(B) revealed its N to be involved in intramolecular H-bonding to the P3 valine NH while its aromatic O and carbonyl O were H-bonded to Asn165 and Ser128, respectively (Figure 1B). This intricate H-bonding network, although originally optimized for the HRV 3C protease, seemed coincidentally well suited for the EV71 3C protease as both viral proteases shared a relatively high (43%) sequence identity. Indeed, our first P4 analog, with an acetyl N-cap (compound **20**) exhibited a 1.5-fold decrease in inhibitory activity compared with compound **2** (9.5 ± 0.7 versus $6.2 \pm 0.6 \mu\text{M}$; Table 1) and we attributed this to the loss of intermolecular H-bonding interactions with Asn165 which were present for the 5-methylisoxazole-3-carbonyl N-cap (Figure 1B). Interestingly, replacing the acetyl with an *iso*-propyl moiety (compound **21**) did not alter inhibitory activity significantly when compared with compound **2** (IC₅₀ value 7.2 ± 0.6 versus $6.2 \pm 0.6 \mu\text{M}$; Table 1). This was postulated to be due to hydrophobic interactions between the *iso*-propyl and the phenyl group of Phe170 located in the S4 subsite (Figure 1F). Replacing the N-cap with phenyl and the larger naphthalene moieties (compounds **22–25**) resulted in less potent inhibitors (IC₅₀ values ranging from 12.9 to 33.3 μM; Table 1), suggesting that larger ring systems were unsuitable for the protease's S4 subsite.

We postulated this to be due to steric hindrance caused by Asn165 located at the edge of the S4 subsite. On this premise, we focused our attention to 5-membered isoxazole analogs (compounds **26–31**; Table 1). The 5-membered 3-furoate moiety of compound **26** exhibited a 1.5-fold decrease in inhibitory activity compared with compound **2** (9.3 ± 0.7 versus $6.2 \pm 0.6 \mu\text{M}$, respectively) and was suspected to be due to the loss of the intramolecular H-bonding interaction between the P4 aromatic N and the backbone amide NH of the P3 valine (Figure 1B). Compound **27** with a 2-furoate moiety suffered a more than 2-fold decrease in inhibitory activity compared to compound **2** (IC₅₀ value 16.1 ± 1.9 versus $6.2 \pm 0.6 \mu\text{M}$, respectively; Table 1) and this was attributed to the loss of H-bonding to Asn165 located at the edge of the S4 subsite. Intriguingly, removing the 5-methyl group from the P4 isoxazole (compound **28**; Table 1) did not significantly affect its IC₅₀ value when compared with compound **2** (7.0 ± 0.9 versus $6.2 \pm 0.6 \mu\text{M}$, respectively; Table 1), suggesting that the isoxazole's methyl group did not play a significant role in hydrophobic interactions in the S4 subsite. Indeed, replacing the methyl group with longer and bulkier alkyl groups did not alter IC₅₀s significantly (compounds **29–31**; Table 1), suggesting that the potential for further P4 optimization might be limited.

Conclusions

EV71 is a highly infectious pathogen primarily responsible for HFMD, particularly in children. To date, there are no effective antiviral drugs to treat this disease^{2,6}. The EV71 3C protease is

deemed an attractive drug target due to its role in viral polyprotein processing. Rupintrivir, a peptide-based HRV 3C inhibitor, has been shown to inhibit EV71 3C protease^{8–10}. As Rupintrivir was originally designed to inhibit the HRV 3C protease, we postulated that there could be room for further optimization against the EV71 protease. Our SAR study using Rupintrivir analogs identified compound **9** to be the most potent inhibitor. Compound **9** contained a P2 ring-constrained phenylalanine analog that was two-fold more potent than Rupintrivir in our protease inhibition assay (IC₅₀ value 3.4 ± 0.4 versus 7.3 ± 0.8 μM, respectively). This suggested that employing geometrically constrained residues was a plausible strategy to improve the inhibitory activities of peptide-based protease inhibitors and should provide valuable insights into the design of future peptide-based antivirals against HFMD.

Declaration of interest

The authors report that they have no conflicts of interest. We thank A*STAR Biomedical Research Council for financial support.

References

- Whitton JL, Cornell CT, Feuer R. Host and virus determinants of picornavirus pathogenesis and tropism. *Nat Rev Microbiol* 2005;3:765–76.
- Wu KX, Ng MM-L, Chu JJH. Developments towards antiviral therapies against enterovirus 71. *Drug Discov Today* 2010;15:1041–51.
- McMinn PC. An overview of the evolution of enterovirus 71 and its clinical and public health significance. *FEMS Microbiol Rev* 2002;26:91–107.
- Rhoades RE, Tabor-Godwin JM, Tsueng G, Feuer R. Enterovirus infections of the central nervous system. *Virology* 2011;411:288–305.
- Yang F, Ren L, Xiong Z, et al. Enterovirus 71 outbreak in the People's Republic of China in 2008. *J Clin Microbiol* 2009;47:2351–2.
- Shang L, Xu M, Yin Z. Antiviral drug discovery for the treatment of enterovirus 71 infections. *Antiviral Res* 2013;97:183–94.
- Norder H, De Palma AM, Selisko B, et al. Picornavirus non-structural proteins as targets for new anti-virals with broad activity. *Antiviral Res* 2011;89:204–18.
- Kuo CJ, Shie JJ, Fang JM, et al. Design, synthesis, and evaluation of 3C protease inhibitors as anti-enterovirus 71 agents. *Bioorg Med Chem* 2008;16:7388–98.
- Lu G, Qi J, Chen Z, et al. Enterovirus 71 and coxsackievirus A16 3C proteases: binding to rupintrivir and their substrates and anti-hand, foot, and mouth disease virus drug design. *J Virol* 2011;85:10319–31.
- Wang J, Fan T, Yao X, et al. Crystal structures of enterovirus 71 3C protease complexed with rupintrivir reveal the roles of catalytically important residues. *J Virol* 2011;85:10021–30.
- Schechter I, Berger A. On the size of the active site in proteases. I. Papain. *Biochem Biophys Res Commun* 1967;27:157–62.
- Binford SL, Maldonado F, Brothers MA, et al. Conservation of amino acids in human rhinovirus 3C protease correlates with broad-spectrum antiviral activity of rupintrivir, a novel human rhinovirus 3C protease inhibitor. *Antimicrob Agents Chemother* 2005;49:619–26.
- Matthews DA, Dragovich PS, Webber SE, et al. Structure-assisted design of mechanism-based irreversible inhibitors of human rhinovirus 3C protease with potent antiviral activity against multiple rhinovirus serotypes. *Proc Natl Acad Sci USA* 1999;96:11000–7.
- Patick AK, Binford SL, Brothers MA, et al. In vitro antiviral activity of AG7088, a potent inhibitor of human rhinovirus 3C protease. *Antimicrob Agents Chemother* 1999;43:2444–50.
- Patick AK. Rhinovirus chemotherapy. *Antiviral Res* 2006;71:391–6.
- Zhang X, Song Z, Qin B, et al. Rupintrivir is a promising candidate for treating severe cases of enterovirus-71 infection: evaluation of antiviral efficacy in a murine infection model. *Antiviral Res* 2013;97:264–9.
- Wang QM, Johnson RB, Cox GA, et al. A continuous colorimetric assay for rhinovirus-14 3C protease using peptide *p*-nitroanilides as substrates. *Anal Biochem* 1997;252:238–45.
- Poulie CBM, Bunch L. Heterocycles as nonclassical bioisosteres of α-amino acids. *ChemMedChem* 2013;8:205–15.
- Kaminski GA, Friesner RA, Tirado-Rives J, Jorgensen WL. Evaluation and reparametrization of the OPLS-AA force field for proteins via comparison with accurate quantum chemical calculations on peptides. *J Phys Chem B* 2001;105:6474–87.
- Polak E, Ribière G. Note on the convergence of methods of conjugate directions. *Recherche opérationnelle, Série Rouge* 1969;16:35–43.
- Hasel W, Hendrickson TF, Still WC. A rapid approximation to the solvent accessible surface areas of atoms. *Tetrahedron Comput Methodol* 1988;1:103–16.

Supplementary material available online
Supplementary data